Available online at www.sciencedirect.com
ScienceDirect
Geochimica et Cosmochimica Acta 70 (2006) 6016–6031
Geochimica
www.elsevier.com/locate/gca

$^{40}Ar/^{39}Ar$ dating of Apollo 12 regolith: Implications for the age of Copernicus and the source of nonmare materials

Fernando Barra [a,b,*], Timothy D. Swindle [a,c], Randy L. Korotev [d], Bradley L. Jolliff [d], Ryan A. Zeigler [d], Eric Olson [c]

[a] Department of Geosciences, University of Arizona, Tucson, AZ 85721, USA
[b] Instituto de Geologia Economica Aplicada, Universidad de Concepcion, Chile
[c] Lunar and Planetary Laboratory, University of Arizona, Tucson, AZ 85721, USA
[d] Department of Earth and Planetary Sciences and McDonnell Center for the Space Sciences, Washington University, St. Louis, MO 63130, USA

Received 27 January 2006; accepted in revised form 20 September 2006

Abstract

Twenty-one 2–4 mm rock samples from the Apollo 12 regolith were analyzed by the $^{40}Ar/^{39}Ar$ geochronological technique in order to further constrain the age and source of nonmare materials at the Apollo 12 site. Among the samples analyzed are: 2 felsites, 11 KREEP breccias, 4 mare-basalt-bearing KREEP breccias, 2 alkali anorthosites, 1 olivine-bearing impact-melt breccia, and 1 high-Th mare basalt. Most samples show some degree of degassing at 700–800 Ma, with minimum formation ages that range from 1.0 to 3.1 Ga. We estimate that this degassing event occurred at 782 ± 21 Ma and may have been caused by the Copernicus impact event, either by providing degassed material or by causing heating at the Apollo 12 site. $^{40}Ar/^{39}Ar$ dating of two alkali anorthosite clasts yielded ages of 3.256 ± 0.022 Ga and 3.107 ± 0.058 Ga. We interpret these ages as the crystallization age of the rock and they represent the youngest age so far determined for a lunar anorthosite. The origin of these alkali anorthosite fragments is probably related to differentiation of shallow intrusives. Later impacts could have dispersed this material by lateral mixing or vertical mixing.

1. Introduction

Although the lunar samples collected from the Apollo and Luna missions in the 1960s and 1970s represent an incomplete sampling of lunar geology, the samples have provided valuable information in understanding the magmatic and impact events that have affected the Moon. The Moon has preserved most of its magmatic and impact history since its origin ~4.5 billion years ago, unlike Earth, where the earliest records of these processes have been erased through plate tectonics and crustal recycling. Thus, the Moon provides important information to understand the early history of the Earth–Moon system.

Lunar samples have been studied extensively for more than three decades and have provided insights on lunar geochemistry and geochronology. Compared to our understanding of lunar geochemistry, which has increased substantially during the last decade with the Lunar Prospector and Clementine missions and lunar meteorites, the absolute chronology of lunar events is sparse. To properly assess the different processes involved in the evolution of the Moon, our understanding of lunar geochemistry should be better coupled with geochronological studies.

The Apollo 12 landing site (Fig. 1) in Oceanus Procellarum is on a volcanic plain (Mare Insularum) composed of low-Ti mare basalts that cover nonmare material of the Fra Mauro or Alpes Formations, which are deposits of Imbrium ejecta (Wilhelms, 1987). Exposures of nonmare material occur within 50 km of the site (Jolliff et al., 2000). Three large craters lie north of the site (Fig. 1A): Copernicus (400 km to rim), the Eratosthenian Reinhold crater (200 km) and the Upper Imbrian Lansberg (100 km) crater. The Apollo 12 sample suite consists mainly of four classes

* Corresponding author. Fax: +1 520 621 2672.
E-mail address: fbarra@email.arizona.edu (F. Barra).

0016-7037/$ - see front matter © 2006 Elsevier Inc. All rights reserved.
doi:10.1016/j.gca.2006.09.013

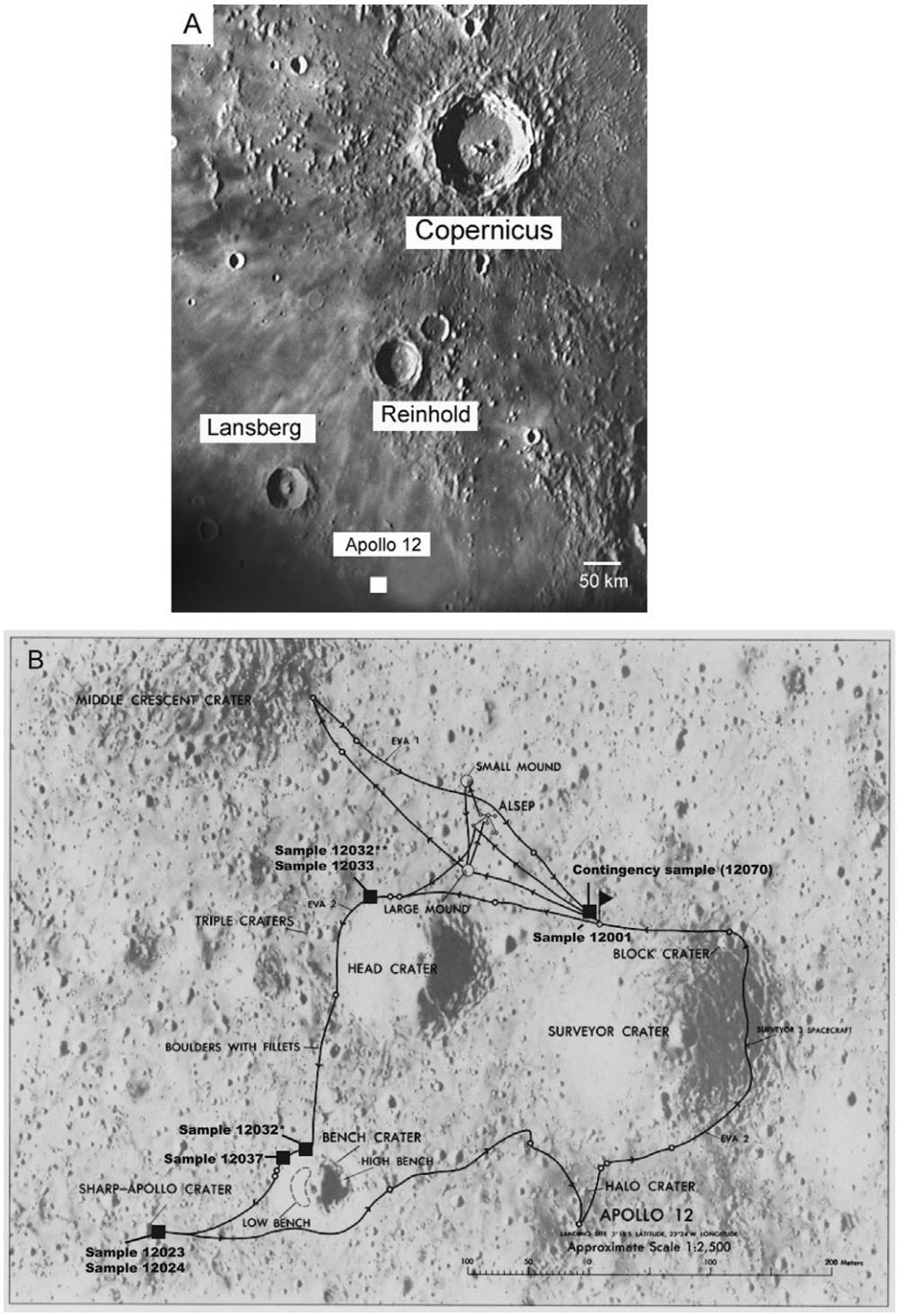

Fig. 1. (A) Location of the Apollo 12 landing site. Also shown are the major craters Copernicus (93 km diameter), Reinhold (48 km diameter) and Lansberg (39 km diameter). (B) Apollo 12 traverses showing the locations of the lunar samples discussed in this study. *Denotes reported location of sample 12032; **denotes proposed alternative location of sample 12032.

of material (Fig. 2): (1) three varieties of low-Ti mare basalt, all with low concentrations of Th, (2) a variety of glassy and crystalline breccias of noritic composition with very high concentrations of Th and other incompatible elements, (3) uncommon to rare lithologies, mainly alkali anorthosites and norites, felsites, and material from the feldspathic highlands, and (4) regolith and breccias composed of all of the other three classes of material. The Th-rich glasses and breccias of Apollo 12 were the first material to which the term KREEP was applied (Hubbard et al., 1971), and we will refer to them here generically as "KREEP breccias".

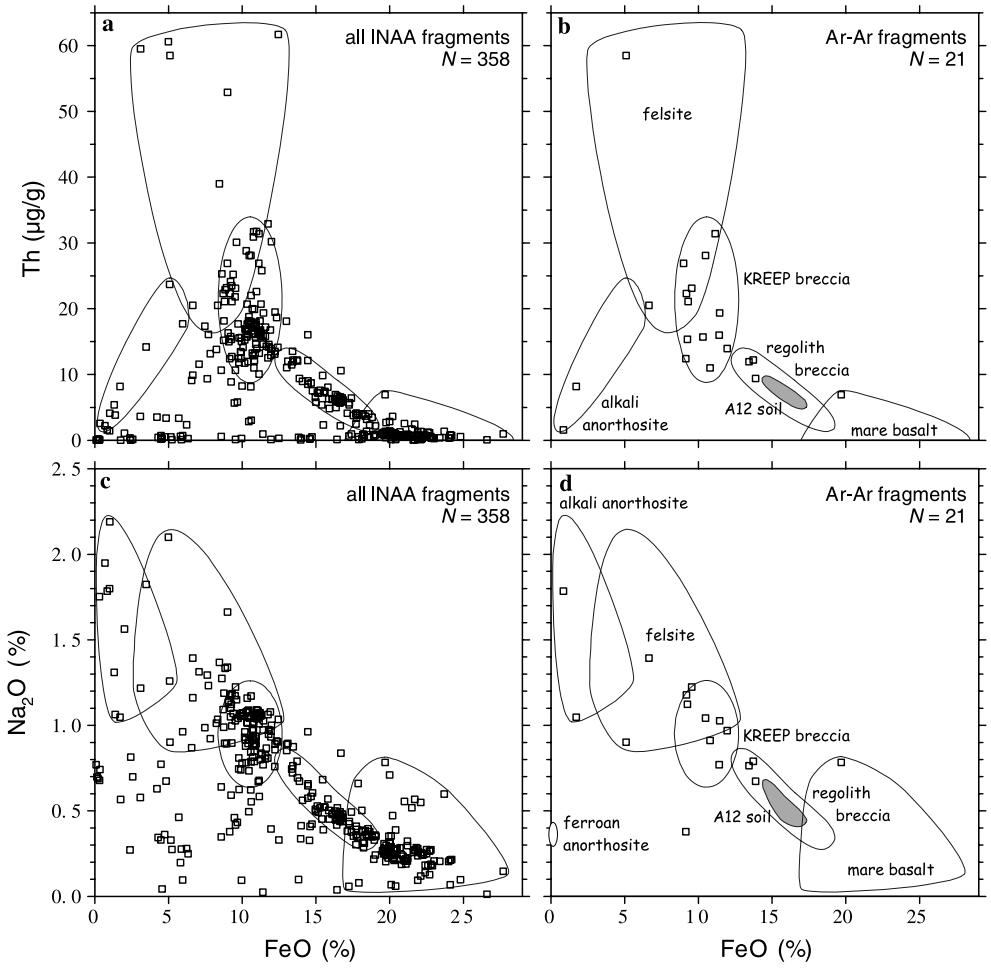

Fig. 2. Compositional classification diagrams for Apollo 12 lithic fragments of this study. (a) Th and FeO concentrations in all fragments analyzed by neutron activation. Most points that plot at intermediate FeO and ~0 Th are for unrepresentative fragments of mare basalt that contain an excess of plagioclase. (b) The subset of fragments analyzed by $^{40}Ar/^{39}Ar$ geochronology. (c and d) Similar plots for Na_2O and FeO concentrations.

The geochemistry of the Apollo 12 mare basalts is well studied (e.g., Neal et al., 1994) and geochronological investigations using different isotopic systems such as K–Ar, $^{40}Ar/^{39}Ar$, Rb–Sr, and Sm–Nd, have yielded ages ranging from 3.1 to 3.3 Ga (e.g. Compston et al., 1971; Papanastassiou and Wasserburg, 1971; Turner, 1971; Stettler et al., 1973; Alexander and Davis, 1974; Horn et al., 1975; Nyquist et al., 1977; Nyquist et al., 1979; Nyquist et al., 1981). Most geochemical and geochronological studies on the nonmare materials of the Apollo 12 site were done within 10 years of the mission (July, 1971). Alkali-suite samples have yielded ages between 3.8 and 4.0 Ga (e.g., Lunatic Asylum, 1970; Turner, 1971; Shih et al., 1993; Meyer et al., 1996), whereas $^{40}Ar/^{39}Ar$ geochronology on ropy glasses from samples 12032/12033 (Eberhardt et al., 1973; Alexander et al., 1976; Bogard et al., 1992) consistently provided ages of ~800 Ma. Similarly, a single lunar granite fragment from sample 12033 also yielded a $^{40}Ar/^{39}Ar$ age of 800 ± 15 Ma (Bogard et al., 1994). All these ~800 Ma ages have been interpreted as the age of the Copernicus crater, or as a reset age in the case of the granite fragment from sample 12033, caused by the Copernicus impact since a ray from this crater crosses the landing site. This work is part of a broader study to characterize the nonmare components of the Apollo 12 regolith and interpret their origin in a modern context. The approach in the geochemical investigation is a modification of one used in the past for samples from other Apollo landing sites (Jolliff et al., 1991, 1996; Korotev and Rockow, 1995; Korotev, 1997; Zeigler et al., 2006) wherein the chemical composition of several hundred lithic fragments from 2 to 4 mm grain-size fraction of the regolith is determined by INAA (instrumental neutron activation analysis), which is nondestructive. A subset of the samples, selected on the basis of composition, is then characterized by standard petrographic techniques or by determination of bulk major-element composition. Unusual or unique samples can be studied further by other techniques (e.g., Jolliff, 1991). For the present study, we included monitors required for $^{40}Ar/^{39}Ar$ geochronological analysis with the samples during the neutron irradiation for INAA. Preliminary results of the compositional analysis were reported in abstracts (Korotev et al., 2000, 2002). Here, we present new $^{40}Ar/^{39}Ar$ geochronological data on 21 selected samples in order to further constrain the age

and source of these materials and to provide insights on the processes that have affected the rocks at the Apollo 12 location. Although we expected to be dating crystallization ages in most cases, it became clear from our data that instead we have found ubiquitous evidence for one or more late impact events, most likely Copernicus.

2. Sample selection

Each of the samples of this study is a lithic fragment that we hand-picked from 2 to 4 mm grain-size fractions of Apollo 12 regolith samples at the astromaterials curation facility of the NASA Johnson Space Center. The selection process favored large, crystalline, nonmare fragments, although numerous mare basalts were included for completeness (Fig. 2). For geochronology, a small subset of fragments was selected on the basis of their composition (Table 1). Most are nonmare materials, although we included one mare basalt of unusual composition and two fragments for which the compositions are consistent with regolith breccias.

The 21 fragments selected for this study derive from six regolith samples. Sample 12001 was taken near the lunar module, samples 12023 and 12024 were taken near Sharp crater, whereas samples 12032 and 12033 were collected on the north rim of Bench crater and from the bottom of a 15 cm deep trench inside the rim of Head crater, respectively (Shoemaker et al., 1970; Warner, 1970) (Fig. 1B). Korotev et al. (2000) questioned the location of sample 12032, however, and proposed an alternate location on the north rim of Head crater based on a similar chemical composition with sample 12033. Hence, both samples 12032 and 12033 were likely collected from the same trench at Head crater (Fig. 1B). Sample 12037 was collected on the north rim of Bench crater and sample 12070 is part of the contingency sample (Warner, 1970).

3. Methodology

For INAA and $^{40}Ar/^{39}Ar$ geochronology, samples were irradiated at the University of Missouri Research Reactor along with MMhb-1 hornblende, CaF_2, and K_2SO_4 salts for a duration of 24 or 36 h in a thermal neutron flux of 5.15×10^{13} cm^{-2} s^{-1}. For Ar geochronology, hornblende was used as a neutron flux monitor and CaF_2 and K_2SO_4 for correction of reactor-induced interferences on Ca and K, respectively. The INAA data reported in Fig. 2 required six separate neutron irradiations; however, the subset of samples discussed in this study were irradiated in three different batches (W334, W335, and W337) and then analyzed by INAA followed by Ar geochronology. Samples 12033,634-06, 12037,225-03, and 12023,146-02 were irradiated in batch W334 with a J factor of 0.0018886 ± 0.0000052, whereas samples 12001,912-02, 12001,907-05, 12033,634-18, 12032,366-41, 12032,366-30, 12033,634-04, 12033,634-15, 12033,634-24, 12033,634-07, 12001,911-01, 12032,366-13, 12033,634-26, 12023,145-03, 12070,882-14, and 12070,882-02 in batch W335, with a J factor of 0.00287 ± 0.00015. Samples 12024,074-04, 12032,366-18, and 12032,366-07 were all irradiated in batch W337 and the J factor was 0.00192 ± 0.00013.

For INAA, samples were radioassayed at Washington University by γ-ray spectrometry four times between 6 and 30 days following the irradiation to determine concentrations of 27 major, minor, and trace elements (Table 1; Jolliff et al., 1991; Jolliff et al., 1996).

For Ar geochronology, samples were analyzed at the University of Arizona noble gas laboratory following the procedure described by Swindle and Olson (2004). Each sample was degassed in a series of temperature extractions (steps) using a resistance-heated furnace and the isotopic composition of the released argon was measured on a VG5400 mass spectrometer by ion counting using an electron multiplier. Data corrections include system blanks, radioactive decay, reactor-induced interferences, cosmic-ray spallation, and solar wind. Blanks are run at room temperature at the start of every day and between samples. Additionally, "hot" blanks are run with the furnace heated to a temperature of 1550 °C. Blank corrections are based on an average of blank runs in the same time period as the sample analysis. Typical blank averages in 10^{-11} cm^3 STP are $^{40}Ar = 24.80 \pm 3.72$, $^{39}Ar = 9.6 \pm 1.4$, $^{38}Ar = 3.4 \pm 0.5$, $^{37}Ar = 5.2 \pm 0.8$, and $^{36}Ar = 17.1 \pm 2.6$. Corrections for radioactive decay of ^{39}Ar are usually minor due to its relatively high half-life (269 years), but can be significant for ^{37}Ar because of its much shorter half-life (35 days).

Besides the formation of ^{39}Ar from ^{39}K in the nuclear reactor, a series of additional reactions occur. These interfering reactions, or reactor-induced interferences, are a function of the reactor facility and total irradiation time. The primary interfering reactions are $^{40}K \rightarrow {}^{40}Ar$, $^{40}Ca \rightarrow {}^{36}Ar$, $^{40}Ca \rightarrow {}^{37}Ar$, $^{42}Ca \rightarrow {}^{39}Ar$, and $^{38}Cl \rightarrow {}^{38}Ar$. In addition to the interfering reactions that produce argon isotopes, there is Ar that is produced by cosmic-ray spallation. The interaction of high-energy particles with the lunar surface produces the same reactions that occur within the nuclear reactor resulting in ^{36}Ar, ^{38}Ar, and ^{40}Ar from calcium- and potassium-bearing minerals. The amount of Ar produced by cosmic-ray spallation that is subtracted from the sample is determined by deconvolving the proportion of ^{36}Ar from spallation and solar wind (Cohen, 2000). These two components, cosmic-ray spallation and solar wind, have known $^{38}Ar/^{36}Ar$ ratios of 1.54 and 0.188, respectively (Eberhardt et al., 1972; Hohenberg et al., 1978) and hence the contribution of each component can be determined. In some cases, after subtraction of argon produced by cosmic-ray spallation there is still some ^{36}Ar and ^{38}Ar left. These remaining argon isotopes are assumed to have been implanted on the uppermost layer (few millimeters thick) of the lunar surface by the solar wind, which has a $^{36}Ar/^{38}Ar$ ratio of 5.26 ± 0.00005 (Eberhardt et al., 1972). Although this $^{36}Ar/^{38}Ar$ ratio is well-derived, this isotopic ratio can undergo significant fractionation during diffusion loss from grain surfaces on the moon, and a range

Table 1
Results of instrumental neutron activation analysis

Sample	AZ ID	WU ID	Chem. class	Na_2O (%)	CaO (%)	Sc (μg/g)	Cr (μg/g)	FeO (%)	Co (μg/g)	Ni (μg/g)	Rb (μg/g)	Sr (μg/g)	Zr (μg/g)	Cs (μg/g)	Ba (μg/g)	La (μg/g)	Ce (μg/g)
12001,912 02	L01	335.030	Felsite	0.90	2.6	8.1	34	5.10	3.6	97	250	76	1090	4.9	2970	75.1	175
12032,366 07	F	337.033	Felsite	1.39	6.2	17.5	790	6.65	11.7	60	83	210	980	3.2	7260	46.4	118
12023,145 03	L15	335.117	KREEP	0.97	13.5	29.0	1650	11.95	24.6	120	8	190	1070	0.51	860	79.0	204
12032,366 13	L13	335.134	KREEP	1.18	10.6	17.7	770	9.19	30.6	290	9	230	1670	0.52	1280	122.0	308
12032,366 30	L06	335.140	KREEP	1.22	9.4	21.0	1245	9.55	16.8	45	46	170	1080	1.6	1780	84.6	215
12033,634 04	L08	335.014	KREEP	1.03	10.8	28.7	1560	11.45	22.0	90	20	230	1270	0.75	1130	94.2	243
12033,634 07	L11	335.108	KREEP	1.12	11.9	21.9	1120	9.26	16.8	<110	17	260	1280	0.86	970	87.1	222
12033,634 15	L09	335.113	KREEP	1.08	13.3	26.0	1395	10.3	18.6	<120	14	210	1130	0.64	1050	97.5	253
12033,634 24	L10	335.017	KREEP	1.34	11.1	17.5	780	8.99	17.1	80	16	190	1930	1.00	770	130.0	325
12033,634 26	L14	335.018	KREEP	1.19	10.9	16.5	740	9.30	37.1	350	26	160	1400	0.96	1360	99.4	252
12037,225 03	L07	334.033	KREEP	1.04	11.5	23.2	790	10.5	17.8	130	24	200	2490	1.0	1290	158.0	399
12070,882 14	L16	335.041	KREEP	0.77	11.1	19.8	1375	11.4	42.6	480	8	190	1020	0.45	645	87.6	225
12033,634 18	L04	335.016	KREEP	1.01	12.3	23.6	880	11.15	16.8	120	<20	210	2350	0.66	1560	176.0	442
12001,911 01	L12	335.012	K–MB	0.79	11.1	32.5	2110	13.7	31.2	100	<20	180	950	0.55	730	68.5	176
12023,146 02	L17	334.020	K–MB	0.76	11.2	32.8	1890	13.4	27.0	100	8	200	960	0.48	730	67.3	173
12024,074 04	46	337.146	K–MB	0.91	12.3	31.1	1590	10.8	16.6	<130	<21	200	920	0.4	670	60.6	158
12070,882 02	L18	335.037	K–MB	0.67	11.2	34.5	2110	13.9	31.8	130	<15	170	790	0.42	650	54.0	139
12032,366 18	H	337.030	MB	0.78	12.7	52.5	1355	19.7	30.6	<80	<12	270	600	0.31	500	41.2	106
12032,366 41	L05	335.146	Ol-IMB	0.38	10.7	9.2	1360	9.15	32.2	230	<5	180	979	0.22	490	77.7	200
12001,907 05	L03	335.032	AlkAn	1.05	16.4	5.1	330	1.72	4.9	30	<3	352	1250	0.17	680	54.2	137
12033,634 06	L02	334.010	AlkAn	1.79	15.8	2.1	50	0.84	1.0	<20	1	455	74	0.07	440	22.8	52
Uncertainty (%)				1	5	1	1	1	1	25	20	15	4	10	2	1	1

Sample	AZ ID	WU ID	Chem. class	Nd (μg/g)	Sm (μg/g)	Eu (μg/g)	Tb (μg/g)	Yb (μg/g)	Lu (μg/g)	Hf (μg/g)	Ta (μg/g)	Ir (ng/g)	Au (ng/g)	Th (μg/g)	U (μg/g)	Mass (mg)
12001,912 02	L01	335.030	Felsite	75	23.1	1.58	6.38	55.9	8.15	34.1	10.0	<2.0	<3.0	58.5	19.0	9.2
12032,366 07	F	337.033	Felsite	65	19.4	3.29	4.23	20.8	2.97	24.5	3.80	<4.0	<6.0	20.5	8.0	15.7
12023,145 03	L15	335.117	KREEP	117	35.0	3.09	7.13	25.4	3.48	26.0	3.33	<7.0	<10.0	14.0	3.8	13.6
12032,366 13	L13	335.134	KREEP	181	52.5	4.00	10.7	38.3	5.25	40.1	4.72	8.7	<14.0	22.3	6.2	14.5
12032,366 30	L06	335.140	KREEP	121	35.1	2.45	7.46	31.0	4.26	26.1	4.55	<5.0	<8.0	23.1	6.4	15.4
12033,634 04	L08	335.014	KREEP	138	41.6	3.20	8.54	30.9	4.25	31.9	4.11	<6.0	<25.0	19.4	5.5	11.0
12033,634 07	L11	335.108	KREEP	126	37.9	3.61	7.71	27.5	3.74	31.1	3.52	<8.0	<12.0	15.4	4.3	13.0
12033,634 15	L09	335.113	KREEP	152	44.4	3.35	8.75	29.0	3.95	27.3	3.78	<6.0	<16.0	15.7	4.4	13.0
12033,634 24	L10	335.017	KREEP	190	52.6	3.72	10.2	39.2	5.26	43.9	4.20	5.7	<8.0	26.9	6.2	9.8
12033,634 26	L14	335.018	KREEP	142	41.1	2.27	8.70	32.7	4.45	35.4	4.39	12.3	<10.0	21.1	5.4	10.6
12037,225 03	L07	334.033	KREEP	235	68.0	3.20	13.6	49.0	6.63	57.9	5.8	3.0	<13.0	28.1	8.1	20.3
12070,882 14	L16	335.041	KREEP	133	37.9	2.53	7.75	26.6	3.60	26.3	3.34	12.5	11	16.0	4.1	10.9
12033,634 18	L04	335.016	KREEP	249	73.3	4.31	14.8	55.9	7.60	53.9	6.60	<10.0	<18.0	31.4	8.6	11.5
12001,911 01	L12	335.012	K–MB	99	30.5	2.53	6.14	22.6	3.13	23.1	3.00	<9.0	<17.0	12.2	3.5	12.3
12023,146 02	L17	334.020	K–MB	101	30.1	2.64	6.14	22.1	3.02	23.6	2.83	<6.0	<30.0	11.9	3.3	21.8
12024,074 04	46	337.146	K–MB	91	27.7	2.52	5.63	20.6	2.82	21.4	2.55	<8.0	<9.0	11.0	3.1	8.8
12070,882 02	L18	335.037	K–MB	79	24.4	2.34	5.03	18.9	2.62	19.7	2.31	<10.0	<12.0	9.4	2.8	12.5
12032,366 18	H	337.030	MB	69	20.3	2.90	4.35	15.2	2.11	15.7	1.84	<5.0	<10.0	6.9	1.7	42.0
12032,366 41	L05	335.146	Ol-IMB	116	33.8	2.76	6.59	21.6	2.92	24.7	2.82	<3.0	<7.0	12.4	3.0	13.7
12001,907 05	L03	335.032	AlkAn	83	24.4	4.64	4.87	15.5	2.02	26.2	1.12	<3.0	<4.0	8.2	2.8	11.8
12033,634 06	L02	334.010	AlkAn	28	7.0	6.59	1.18	3.4	0.45	1.8	0.59	<1.3	<3.0	1.6	0.4	17.3
Uncertainty (%)				3	1	1	1	1	1	1	3	25	35	2	5	

All Fe is reported as FeO although some Fe occurs as metal. Uncertainties are one-standard-deviation estimates of analytical precision based mainly on counting statistics. The Washington University (WU) and University of Arizona (AZ) laboratory designations of each fragment are listed in the second and third columns. The chemical classifications are based on plots such as Fig. 2: AlkAn, alkali anorthosite; K–MB, composition consistent with mixture of KREEP and mare basalt; MB, mare basalt; Ol-IMB, olivine-bearing impact melt breccia.

in $^{36}Ar/^{38}Ar$ ratios has been measured in soils and breccias. Variations in the $^{36}Ar/^{38}Ar$ ratio will be particularly significant in low temperature steps (<500 °C) with $^{36}Ar/^{38}Ar$ ratios close to the 5.26 value. These low temperature steps usually yield unreliable age information, mostly due to terrestrial argon contamination and hence we do not assign any relevance to variations in the $^{36}Ar/^{38}Ar$ solar-wind ratio.

The amount of "parentless" ^{40}Ar accompanying solar wind in samples (Eugster et al., 2001) is determined by constructing an isochron diagram to constrain the initial $^{40}Ar/^{36}Ar$ ratio for the high-temperature steps (Fig. 3a and b). As mentioned above, in some cases, low temperature steps yield an $^{40}Ar/^{36}Ar$ ratio close to the terrestrial value (295.5) suggesting contamination by terrestrial argon (Swindle and Olson, 2004). In others they do not fall on an

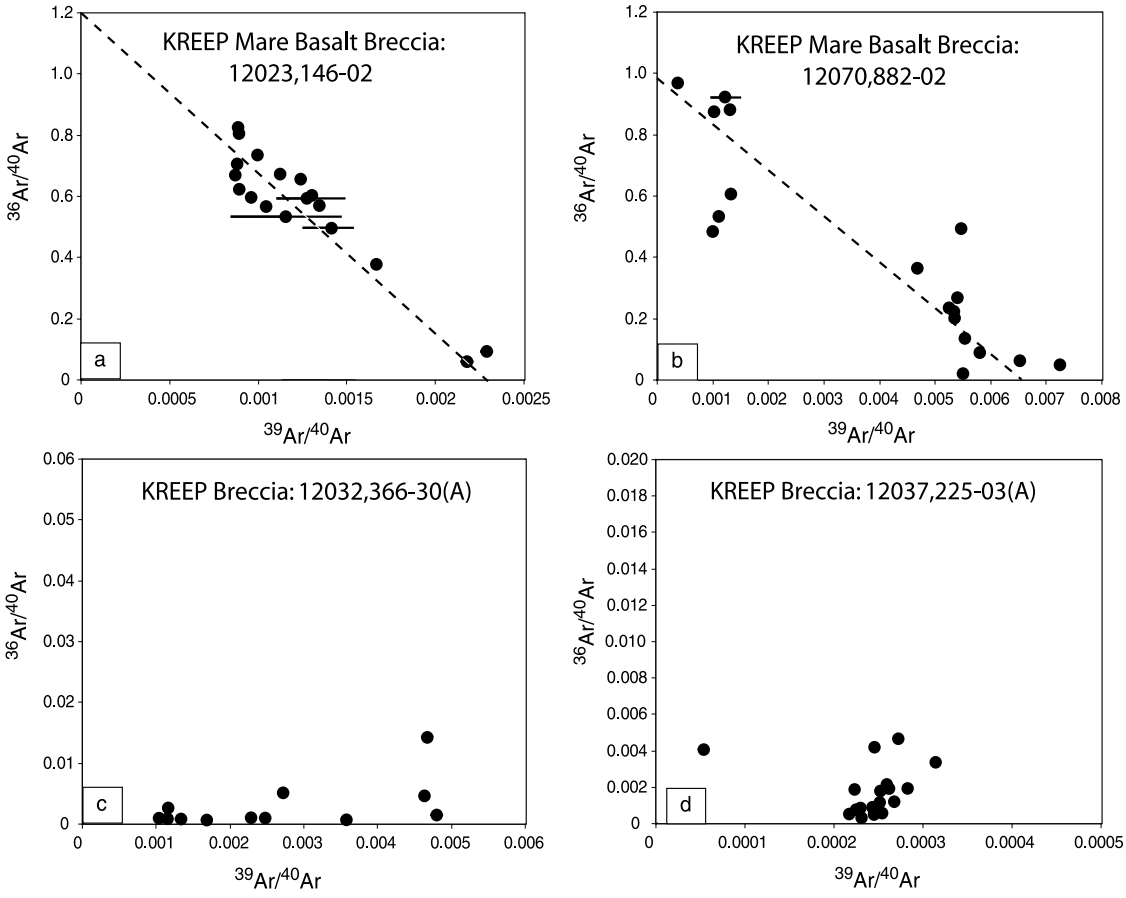

Fig. 3. Isotope correlation diagrams showing two examples of reasonably good correlation (a) and (b), and two examples of poor correlation (c) and (d). The initial $^{40}Ar/^{36}Ar$ determined from the three-isotopes plots for samples 12023,146-02 (a) and 12070,882-02 (b) was 0.8 ± 0.1 and 1.0 ± 0.1, respectively.

isochron (i.e., show a poor correlation, Fig. 3c and d), yielding meaningless apparent ages. In those cases where no reliable $^{40}Ar/^{36}Ar$ was obtained we applied a nominal correction assuming $^{40}Ar/^{36}Ar = 5 \pm 5$, spanning the range expected (Eugster et al., 2001). This correction was applied to samples with ages over 2.5 Ga (sample 12037,225-03), whereas in other cases, where the ages were in the range of 700–800 Ma, we took a $^{40}Ar/^{36}Ar$ of 1 ± 1 value for our correction (i.e., samples 12001,912-02, 12032,366-13, 12032,366-18, 12032,366-30, 12032,366-41, 12033,634-07, 12033,634-15, 12033,634-18, 12033,634-24, and 12033, 634-26). The magnitude of this solar-wind correction is not significant for these samples, since this correction is most relevant in samples that have high contents of ^{36}Ar, and in those particular cases we were able to obtain an initial $^{40}Ar/^{36}Ar$ from the three-isotopes plot.

Although most data reduction was fairly standard, as described in the above section, we used an unusual technique to correct for the ^{39}Ar produced by irradiation of Ca in the reactor, both necessitated and enabled by our specific experimental circumstances.

The most abundant argon product of irradiation of Ca is ^{37}Ar, and since ^{37}Ar is radioactive (with a 35-day half-life) and not produced in significant amounts by any other process in the reactor, most of the ^{37}Ar in an irradiated rock sample will come from Ca. However, because of the short half-life of ^{37}Ar, samples must be analyzed within a few months of irradiation to detect it. The normal technique is to include samples of CaF_2 in the irradiation as monitors of the reactions producing Ar from Ca, particularly of the $^{39}Ar/^{37}Ar$ ratio, which then can be used in conjunction with the ^{37}Ca measured in the sample to determine the amount of Ca-derived ^{39}Ar.

We had CaF_2 monitors in all of our irradiation packages, but could not effectively use the ^{37}Ar because we analyzed some samples two years or more after irradiation, when the ^{37}Ar had decayed to levels comparable to our blanks. However, one of the reasons for the delay was that the samples were analyzed via INAA to determine the abundances of many elements, including Ca. Hence, we know the amount of Ca in the sample we analyzed, so we can determine the $^{39}Ar/[Ca]$ ratio (where the symbol in brackets refers to the elemental abundance) in the CaF_2 for an irradiation, then combine that with the Ca abundance in each sample to determine the total amount of Ca-derived ^{39}Ar in each sample. However, this still does not tell us how much of the ^{39}Ar in each heating step is Ca-derived.

To apportion the Ca-derived ^{39}Ar among the different heating steps, we note that (a) most of the cosmic-ray-spallation ^{36}Ar and ^{38}Ar in Ca-rich lunar samples such as these

come from Ca and (b) lunar samples contain little Cl (which can produce noticeable amounts of ^{38}Ar in irradiated terrestrial samples or meteorites). This means that the ^{36}Ar and ^{38}Ar are basically two-component mixtures of Ca-derived spallation and solar wind, each with known $^{38}Ar/^{36}Ar$ ratios. We determine how much Ca-derived ^{38}Ar each step contains, sum those, and then find what fraction of the total each step contains. Since Ca-derived ^{38}Ar (from spallation) and Ca-derived ^{39}Ar (from irradiation) should occupy the same lattice sites, we can then calculate an amount of Ca-derived ^{39}Ar in each step.

Such a technique would not work for samples (meteoritic or terrestrial) with measurable amounts of ^{38}Ar from Cl, or on Ca-poor samples in which the Ar spallation is not as clearly dominated by Ca, but it appears to work well here (we obtained reasonable agreement on samples for which we did have measurable ^{37}Ar amounts). We are less confident in the technique on a Ca-poor sample (in which the Ar spallation is not dominated by Ca) such as 12001,912-02, but we found on that sample that the low-Ca (and high K) meant that the details of how the correction for Ca-produced ^{39}Ar was done made an insignificant difference in the final calculated apparent ages.

Plateau diagrams were constructed using ISOPLOT (Ludwig, 2001) and here a plateau is defined as three or more consecutive steps that release 60% or more of the ^{39}Ar, with apparent ages overlapping within their 1-σ uncertainties. In some cases, where several various consecutive steps have similar apparent ages but do not conform to a plateau age, a weighted average age is calculated using ISOPLOT (Ludwig, 2001). Although not a plateau age, these weighted average ages are our best estimate of the age in these particular cases. All uncertainties are reported at 1-σ level.

K/Ca histograms for each sample are based on $^{38}Ar_{spallation}/^{39}Ar$ ratios and are normalized to the highest value obtained for the sample. In those cases where we analyzed splits of a single sample, normalization was based on the highest K/Ca ratio obtained from both analyses.

4. Results

Results of INAA show that the Apollo 12 regolith consists of a variety of lithologies (Fig. 2a and c). Most lithic fragments in the 2–4-mm grain-size fraction are mare basalts and KREEP breccias. Also abundant are breccias with compositions intermediate to KREEP impact-melt breccia and mare basalt. Most of these are probably regolith breccias because they have compositions similar to the <1-mm fines (“A12 soil” in Fig. 2). Some, however, particularly those that plot close to the KREEP breccia field of Fig. 2 and are enriched in Sc (Table 1), are probably impact-melt breccias dominated by some form of KREEP but with a component of mare basalt. In the discussion below, such

Table 2
Summary of $^{40}Ar/^{39}Ar$ ages (in Ma) for regolith samples discussed in text. (errors at 1-σ)

Sample	Split	Weight (mg)	Chemical classification	Lower age				Other age		High age				Comments
				Limit	Error	Plateau	Error	Plateau	Error	Limit	Error	Plateau	Error	
12001,912-02	A	0.504	Felsite	767	9					2103	38			
	B	1.375		745	3	769	26			2867	40			
12032,366-07		0.577	Felsite	680	5	685	8			1039	12			
12023,145-03		13.627	KREEP	752	9			1659	61	2045	81			
12032,366-13		14.523	KREEP	700	11	706	6			2349	27			
12032,366-30	A	3.981	KREEP	845	11					2265	42			
	B	2.717		680	39					2003	47			
12033,634-04		11.050	KREEP	770	7	790	13			1208	20			
12033,634-07		13.028	KREEP	755	32			913	24	1311	7			
12033,634-15		13.057	KREEP	765	34	862	38	1425	31	2018	30			
12033,634-24		9.811	KREEP	770	15	792	12			1589	40			
12033,634-26		10.627	KREEP	726	21	788	11			2127	24			
12037,225-03	A	4.595	KREEP	3823	130							3991	25	Little or no resetting at 700–800 Ma
	B	1.253		2337	115							3085	56	Little or no resetting at 700–800 Ma
12070,882-14		10.973	KREEP	2559	89					3829	78			Little or no resetting at 700–800 Ma
12033,634-18		5.476	KREEP	805	2	822	60			2509	109			
12001,911-01		12.327	K–MB	1018	14			1575	33	1917	22			
12023,146-02		21.694	K–MB	981	185			1059	10					
12024,074-04	A	1.241	K–MB	995	27			1054	6	1066	9			
	B	2.398		973	37			1054	31	2869	191			
12070,882-02		12.456	K–MB	426	37	663	17			1640	104			
12032,366-18	A	1.884	Mare basalt	548	21	688	10			2329	48			Involved in later thermal event
	B	0.338		487	41					2736	210			Involved in later thermal event
12032,366-41	A	4.270	KREEP	750	20					3137	80			
	B	5.383		871	48					3597	75			
12001,907-05		11.799	AlkAn	1720	558							3105	58	
12033,634-06		17.307	AlkAn	1561	30							3256	22	

fragments (>30 μg/g Sc) are designated KREEP–mare-basalt breccias (K–MB in Tables 1 and 2). Other minor lithologies include felsite, alkali anorthosite, alkali norite, and plagioclase-rich lithologies derived from the feldspathic highlands. Below we describe results for the 21 samples for which we obtained Ar–Ar data (Fig. 2b and d). The isotopic composition of Ar released and apparent age for each heating step are provided in the electronic annex file EA-1. A summary of results and amounts of sample analyzed is shown in Table 2.

4.1. Felsite 12001,912-02

Sample 12001,912-02 is a felsite (granite) rock fragment. It has low concentrations of FeO, Sc, and Cr, and high concentrations of alkali elements ($K_2O = 8.8$ wt%), Ba, Zr, Hf, Ta, Th, and U (Table 1, Fig. 2), and a shallow V-shaped REE pattern showing enrichment of the HREE, typical of lunar granite (e.g., Jolliff, 1991). Two splits of this sample were analyzed for Ar–Ar geochronology, A and B. In split A, a total of 11 heating steps were made (Fig. 4-1). The first three low temperature steps (extractions) provided meaningless age information, probably due to terrestrial argon contamination. Three consecutive steps released 73% of the ^{39}Ar, with most of it (41%) released in a single step. These three steps have ages between 767 and 910 Ma. Higher temperature steps have a maximum apparent age of ~2.1 Ga, which is probably the lower limit of the crystallization age. In split B eight consecutive steps released ~66% of ^{39}Ar with apparent ages between 745 and 836 Ma. Of these eight extractions, six have apparent ages between 745 and 782 Ma, with 53% ^{39}Ar. A weighted average of these six extractions gave an age of 769 ± 26 Ma (Fig. 4-2). At higher temperatures, steadily increasing ages are associated with increasing extraction temperatures, from 920 to 3143 Ma, with around 33% ^{39}Ar. The pattern suggests a rock with a minimum crystallization age of 2.8 Ga that was mostly, but not completely, degassed around 769 Ma.

4.2. Felsite 12032,366-07

Felsite sample 12032,366-07 shows a pattern of degassing at a recent age and air contamination at the first temperature extraction (Fig. 4-3). Two consecutive extractions at 500 and 650 °C with 41% of the ^{39}Ar give an age of

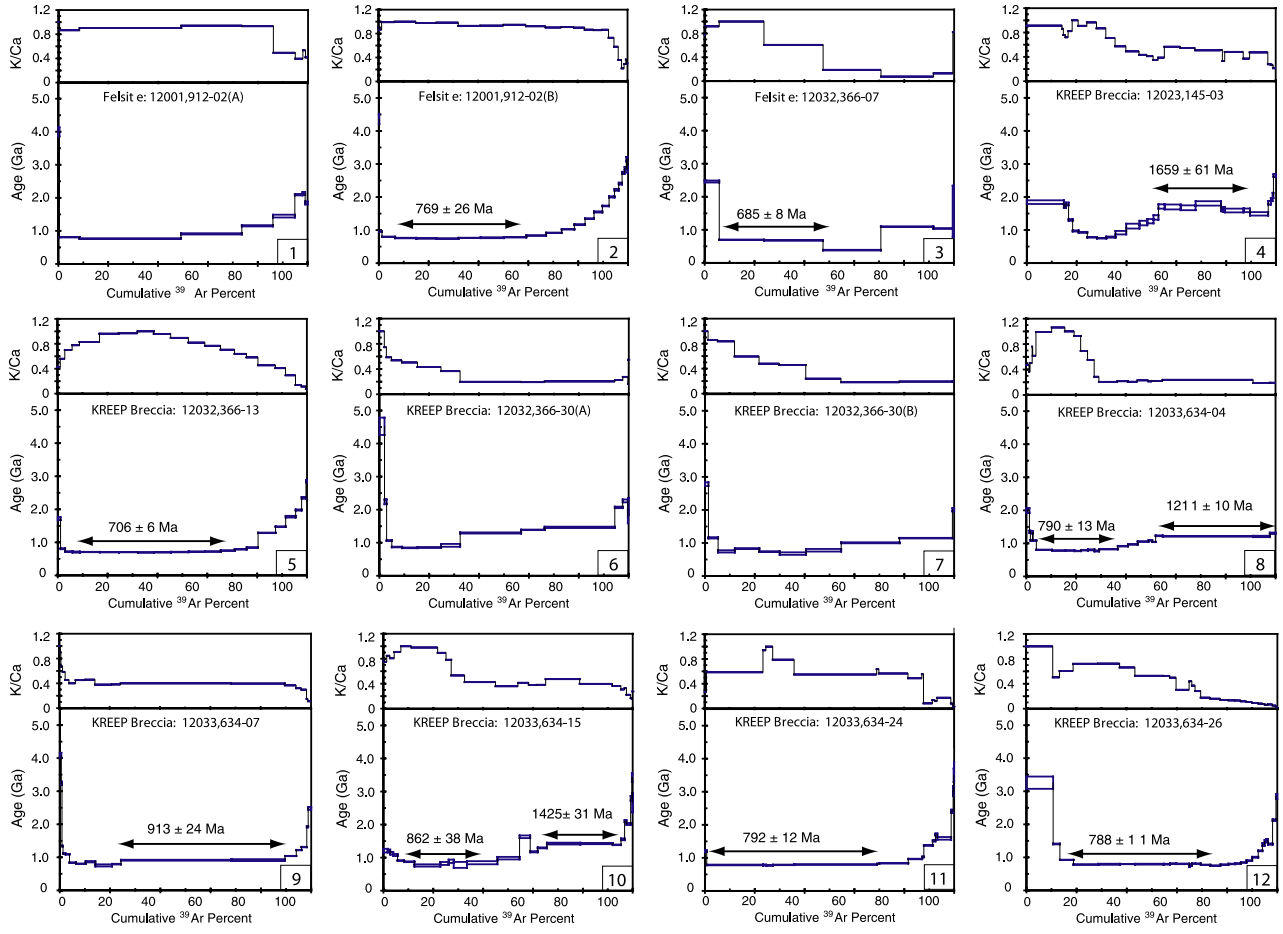

Fig. 4. Plots of apparent $^{40}Ar/^{39}Ar$ age and K/Ca versus fraction of K-derived ^{39}Ar released for whole rock Apollo 12 regolith samples. The "K/Ca ratio" is actually the ratio of ^{39}Ar (produced in the reactor by neutron-capture on K) to ^{38}Ar produced by spallation reactions on Ca, normalized to the highest ratio measured in the sample (see Section 3).

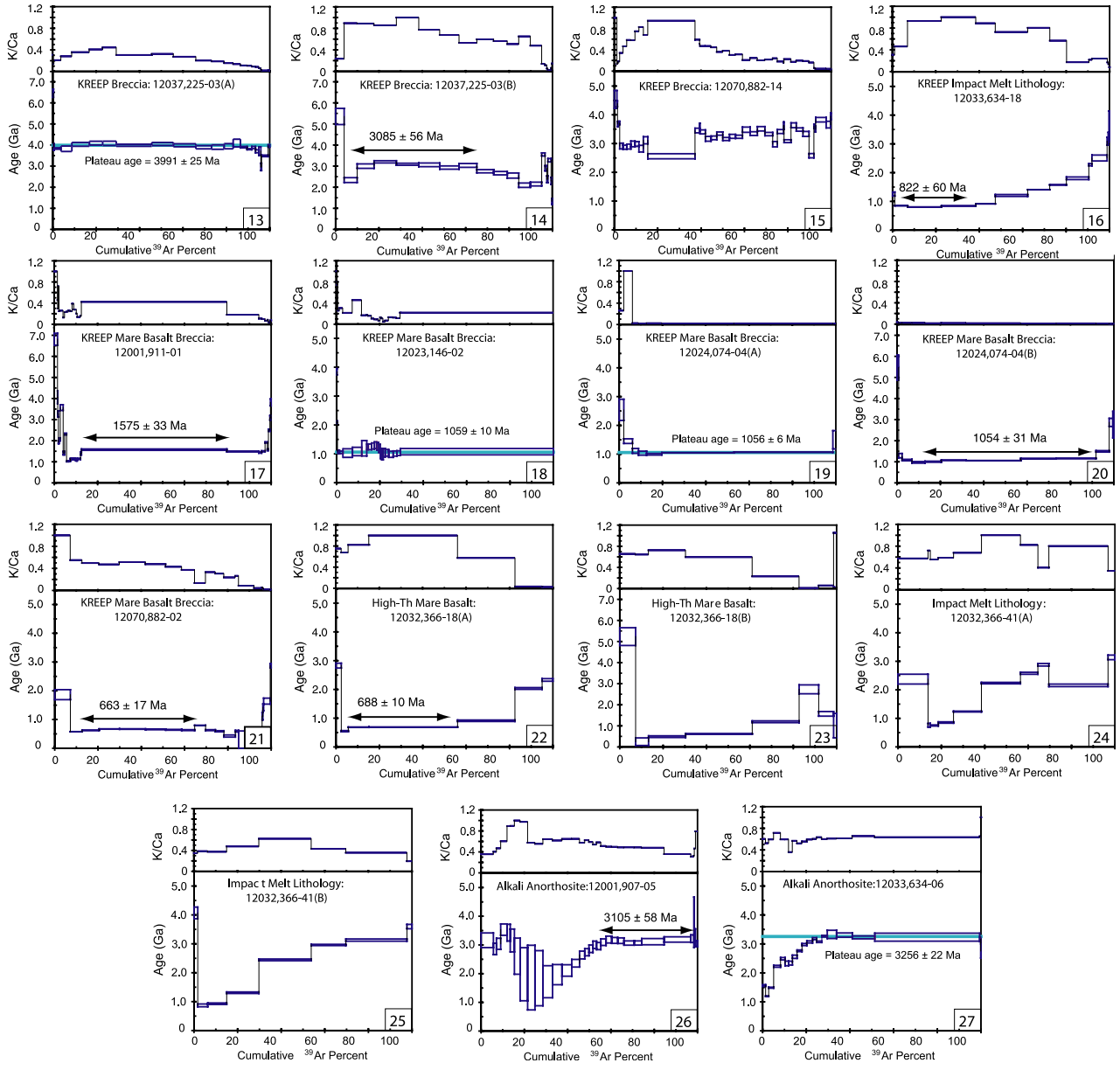

Fig. 4 (*continued*)

685 ± 8 Ma, suggesting that degassing occurred at that time. The highest apparent age is 1039 Ma. A polished section of this sample shows coarse segregations of silica and K–feldspar–silica granophyre, and a mafic, vitrophyric matrix, that penetrates and embays the coarse, felsic crystalline components. Macroscopically, this vitrophyric phase also coated the original rock particle. The matrix may be quenched impact melt, which is consistent with the extensive degassing of this sample.

4.3. KREEP breccia 12023,145-03

Analysis of sample 12023,145-03, which probably contains a minor component of mare basalt (Sc = 29 ppm), showed air contamination at the lowermost temperature steps and steadily decreasing ages at low extraction temperatures (<950 °C), reaching a minimum of 752 ± 9 Ma, followed by increasing ages with increasing temperature steps. Eight consecutive steps with 37% of the ^{39}Ar have ages between ~1.6 and ~1.8 Ga with a weighted average of 1659 ± 61 Ma (Fig. 4-4). The pattern indicates a rock with a formation age of at least ~2.0 Ga (oldest apparent age) and partial degassing at around 750 Ma.

4.4. KREEP breccia 12032,366-13

For fragment 12032,366-13, the same pattern of increasing apparent ages with increasing extraction temperature was observed. Ten consecutive steps, with approximately 62% of ^{39}Ar give a weighted average age of 706 ± 6 Ma

(Fig. 4-5). The oldest apparent age is 2349 Ma and is interpreted as the minimum age of formation, with a partial degassing event at ~700 Ma.

4.5. KREEP breccia 12032,366-30

We analyzed two splits of fragment 12032,366-30. Split A shows an Ar-release pattern with a minimum crystallization age of around 2.2 Ga that was partially degassed at ~845 Ma or later (Fig. 4-6). Split B also shows this pattern, with four consecutive steps, which have ages between 680 and 830 Ma (Fig. 4-7). Two consecutive high-temperature steps, i.e., 1050 and 1150 °C, released more than 40% of ^{39}Ar and have associated ages of 1.0 and 1.1 Ga, respectively. The estimated minimum formation age for this sample is 2.0 Ga.

4.6. KREEP breccia 12033,634-04

Fragment 12033,634-04, which may contain a minor component of mare basalt (29 μg/g Sc, Table 1), shows a pattern of steadily increasing age with increasing extraction temperature, from 783 to 1305 Ma. This pattern includes seven consecutive extractions with 25% of the ^{39}Ar that have a weighted average age of 790 ± 13 Ma. A single high-temperature step (1175 °C) released 36% of the ^{39}Ar and has an apparent age of 1211 Ma (Fig. 4-8). This step falls within the pattern of steadily increasing ages, however, so it probably has no significance beyond that. The overall age pattern is of a rock formed at 1.2–1.3 Ga or earlier and partially degassed around 800 Ma.

4.7. KREEP breccia 12033,634-07

For sample 12033,634-07, the lowest temperature steps show some terrestrial argon contamination and hence the associated ages are not reliable. Sixty-five percent of the ^{39}Ar was released in two consecutive high-temperature extractions (1175 and 1200 °C) that have ages of 913 and 916 Ma, respectively (Fig. 4-9). The overall pattern of this sample is of a rock with a minimum crystallization age of ~1.3 Ga (highest apparent age) that was mostly, but not completely, degassed around 755 Ma. Another possible interpretation is that this sample was strongly degassed at 913 Ma and the slightly younger ages at lower temperatures represent later diffusion loss. This 913 ± 24 Ma age is within error of the 862 ± 38 Ma age for sample 12033,634-15 and might represent a common degassing event.

4.8. KREEP breccia 12033,634-15

The low temperature steps showed evidence of some degree of terrestrial argon contamination. Subsequent higher temperature extractions showed steadily increasing ages with increasing temperature steps, from 780 to ~3.4 Ma. Six consecutive steps with 37% of the ^{39}Ar have ages between 764 and 890 Ma with a weighted average of 862 ± 38 Ma. Two consecutive high-temperature extractions with 26% of the ^{39}Ar yielded a weighted average age of 1425 ± 31 Ma. The pattern indicates a rock with a formation age of at least 2.0 Ga (oldest apparent age) and partial degassing at 860 Ma or later, very possibly 765 Ma or later (Fig. 4-10).

4.9. KREEP breccia 12033,634-24

For sample 12033,634-24, five consecutive steps released 68% of ^{39}Ar with apparent ages between 770 and 799 Ma, with a weighted average of 792 ± 12 Ma (Fig. 4-11). A pattern of steadily increasing ages associated with increasing extraction temperatures is also observed in this sample, from 800 Ma to 3.4 Ga. The pattern is similar to the one described for previous samples, i.e., a rock with a minimum formation age around 1.6 Ga that was degassed ~780 Ma.

4.10. KREEP breccia 12033,634-26

Twenty-nine temperature extractions were performed on sample 12033,634-26. The first three temperature extractions showed evidence for terrestrial argon contamination and did not yield reliable ages. The following 16 consecutive low temperature steps (475–900 °C) with 66% of the ^{39}Ar have ages between 726 and 812 Ma. These steps yield a weighted average of 788 ± 11 Ma (Fig. 4-12). The pattern is of a rock with a minimum formation age around 2.1 Ga that was partially degassed ~790 Ma.

4.11. KREEP breccia 12037,225-03

Two splits of this sample were analyzed, A and B. In split A, a total of 22 heating steps were made. Sixteen consecutive steps with approximately 93% of the ^{39}Ar have apparent ages between 3.8 and 4.0 Ga. Eleven consecutive steps with 83% of ^{39}Ar yielded a plateau age of 3991 ± 25 Ma (Fig. 4-13). This is the oldest age obtained in the analyzed sample set. Split A does not show the degassing pattern observed in the other samples. Surprisingly, >70% of the ^{39}Ar is released by 675 °C—only one other sample (12070,882-02) released as high a fraction that early. Lower ages at the high temperature end suggest a possible recoil effect. Based on an Arrhenius plot (not shown), the activation energy is ~39 kcal/mol. Though higher than some activation energies determined, this is within 2 kcal/mol of samples 12033,634-15 and 12033,634-24, both of which appear to have been almost completely degassed in a later impact. The second split (B) did not yield a plateau age, but six consecutive steps released ~55% of ^{39}Ar with apparent ages between 2.9 and 3.2 Ga and a weighted average of 3085 ± 56 Ma (Fig. 4-14). The two splits had distinctly different K/Ca ratios (Fig. 4-13 and -14). This indicates that the age difference between the fractions is probably caused by mineralogical heterogeneities between the splits.

4.12. KREEP breccia 12070,882-14

We made 41 extraction steps on sample 12070,882-14 but obtained no useful age information from extractions below 500 °C. A single-step extraction released 22% of the ^{39}Ar with an age of 2559 Ma. Overall the ages for this sample range from 2.5 to 3.8 Ga (highest apparent age), with most of the ages between 2.8 and 3.3 Ga (Fig. 4-15).

4.13. KREEP impact-melt lithology 12033,634-18

Sample 12033,634-18, like other fragments classified here as "KREEP," has a composition consistent with a KREEP-rich impact-melt breccia. Sample 12033,634-18 differs, however, in that it appears unbrecciated and is one of a cluster of about 12 rock fragments (of 358 fragments) that have significantly greater concentrations of incompatible elements (e.g., ~30 μg/g Th) than the mean (~17 μg/g; Fig. 2). For comparison, "average high-K KREEP" as defined by Warren (1989) has 22 μg/g Th. Sample 12033,634-18 is similar in composition to the impact-melt breccia lithology in lunar meteorite Sayh al Uhaymir 169 (Gnos et al., 2003). Analysis of sample 12033,634-18 showed that 92% of the ^{39}Ar gave steadily increasing ages with increasing temperature steps, from 805 to ~3.6 Ga (Fig. 4-16). Three consecutive steps with 36% of the ^{39}Ar have ages between 805 and 850 Ma. The pattern indicates a rock with a formation age of at least ~2.5 Ga and degassing around 800 Ma.

4.14. KREEP–mare-basalt breccia 12001,911-01

The composition of sample 12001,911-01 is consistent with a mixture of KREEP and mare basalt, but dominated by KREEP. The rock fragment was glassy or aphanitic with a soil coating. Most of the extractions yielded ages between 1.0 and 1.5 Ga with 67% of the ^{39}Ar released in a single extraction at 1075 °C with an age of 1575 ± 33 Ma (Fig. 4-17).

4.15. KREEP–mare-basalt breccia 12023,146-02

For sample 12023,146-02, a mare-basalt-bearing KREEP breccia, ~99% of the ^{39}Ar corresponds to a plateau age of 1059 ± 10 Ma, with 70% of the ^{39}Ar released in the last temperature extraction (Fig. 4-18). The last extraction was at only 1140 °C, because the furnace burned out at this point, but most samples had released most of their gas by this point, so we suspect our extraction was close to complete.

4.16. KREEP–mare-basalt breccia 12024,074-04

We analyzed two splits of sample 12024,074-04, A and B. The low temperature steps (<400 °C) in split A did not yield reliable age information. Two consecutive extractions at 950 and 1100 °C with around 79% of the ^{39}Ar give ages of 1049 and 1066 Ma, respectively. Overall split A has a plateau age of 1054 ± 6 Ma with 80% of the ^{39}Ar (Fig. 4-19). We were able to make more temperature extraction steps on split B because the sample mass was higher. Again we see low temperature steps with unreliable age information. The lowest apparent age is 973 Ma at an extraction temperature of 600 °C and the highest apparent age is ~2.8 Ga. Around 55% of ^{39}Ar gives a weighted average age of 1054 ± 31 Ma (Fig. 4-20), which is consistent with the age of previous split (A) and could reflect the age of degassing.

4.17. KREEP–mare-basalt breccia 12070,882-02

Sample 12070,882-02 is also a mare-basalt-bearing KREEP breccia. The first temperature step (300 °C) showed terrestrial argon contamination. Around 88% of ^{39}Ar corresponds to ages between 418 and 798 Ma. Five consecutive low temperature extractions from 450 to 575 °C have ages between 631 and 671 Ma, yielding a weighted average of 663 ± 17 Ma (Fig. 4-21). The oldest apparent age is ~1.6 Ga.

4.18. High-Th Mare Basalt 12032,366-18

Sample 12032,366-18 is a crystalline mare basalt that is compositionally unique, with a high concentration of Th (7 μg/g, Jolliff et al., 2005). The Jolliff et al. (2005) study reported that 12032,366-18 is in fact a crystalline mare basalt, and not a mixture of basaltic and KREEPy materials. Split A shows two consecutive steps with 50% ^{39}Ar that have a weighted average age of 688 ± 10 Ma (Fig. 4-22), then increasing ages with increasing extraction temperature, with an oldest apparent age of ~2.3 Ga. This suggests a crystallization age of 2.3 Ga or older and degassing at approximately at 690 Ma. Split B shows air contamination in the lower temperature steps and increasing ages with increasing extraction temperature. A single extraction with 17% of the ^{39}Ar gives an age of ~487 Ma and the following extraction with 30% of ^{39}Ar gives an age of 617 Ma. The oldest apparent age is ~2.7 Ma at an extraction temperature of 1000 °C, followed by an extraction at 1100 °C with an associated age of 1569 Ma, suggesting possible recoil (Fig. 4-23). Since both splits, A and B yielded minimum apparent ages of <550 Ma, it is also possible that this sample was affected by some event slightly later than the pervasive ~700–800 Ma event at the Apollo 12 site.

4.19. Impact melt lithology 12032,366-41

Sample 12032,366-41 has an unusual composition compared to other KREEP-rich samples. It has low Na, Sc, Rb, Cs, and Ba, and its composition is at the low end in terms of incompatible-element enrichment compared to the other KREEP-rich rock fragments. Its low Sc/Cr is

consistent with an olivine-bearing impact-melt breccia. Two splits of this sample were dated. In split A, 14 steps were performed, the first three steps (temperature <550 °C) provide meaningless age information. Sixty percent of the ^{39}Ar gave increasing ages with increasing extraction temperature, from 760 to 2879 Ma, followed by a temperature step that released ~27% of the ^{39}Ar and yielded a younger age of 2156 Ma (Fig. 4-24). This was probably by different phases that degassed at different temperatures. Split B shows steadily increasing ages, which are associated with increasing extraction temperatures, from 870 to 3597 Ma (Fig. 4-25). Taken together, these patterns suggest a rock with a minimum formation age of ~3.6 Ga that was partially degassed ~750 Ma or later. The difference in apparent ages between both splits is probably caused by variable clast content of the fractions or splits.

4.20. Alkali anorthosite 12001,907-05

Sample 12001,907-05 has compositional characteristics similar to those of alkali anorthosite. Under the binocular microscope, it appears to be coarsely crystalline and rich in plagioclase. Glassy areas indicate that this rock has been partially impact melted. Its Ar-release pattern shows decreasing ages associated with the lower temperature steps (<725 °C) and then increasing ages from ~1.9 to 3.2 Ga. Eleven consecutive steps with approximately 68% of the ^{39}Ar have apparent ages between 2.9 and 3.2 Ga that yielded a weighted average of 3105 ± 58 Ma (Fig. 4-26). This rock probably formed around 3.2 Ga and was partially degassed at ~1.7 Ga or more recently. The plateau age is slightly younger than previously reported in Barra et al. (2004) due to a better correction of Ca interferences and solar-wind correction as explained in Section 3.

4.21. Alkali anorthosite 12033,634-06

Sample 12033,634-06 is an alkali anorthosite by virtue of its low concentrations of Fe, Sc, and Cr and high concentrations of Ca, Na, Sr, and Eu. The first three temperature steps show evidence of terrestrial atmospheric contamination. Increasing temperature extractions showed steadily increasing ages from ~1.5 to ~3.3 Ga. Six consecutive high-temperature steps yielded a plateau age of 3256 ± 22 Ma (Fig. 4-27). The Ar-release pattern was distinct from any other sample we analyzed, with most of the ^{39}Ar (48%) released in a single step at 1425 °C, and >77% release at $T > 1250$ °C (no other sample released >5% at $T > 1250$ °C). The pattern indicates a rock that formed around 3256 Ma and was partially degassed at the time of the youngest apparent age (1560 Ma) or more recently. Not surprisingly, given the high release temperature and refractory composition, this sample seems to have been far less affected by later impact events than most of the others.

We determined limits on the cosmic-ray exposure (CRE) ages of all samples, based on the measured amounts of calcium (from INAA) and cosmogenic ^{38}Ar, and upper limits on the production rates (Hohenberg et al., 1978). We will not go into these in detail in this paper (we plan to do so elsewhere), but note that the vast majority of the CRE ages are consistent with exposures beginning during or after the suggested 800 Ma event. The highest minimum CRE age is 940 Ma, and it is the only one >850 Ma. Four samples do have minimum CRE ages 10–30% higher than our preferred Ar–Ar ages for the samples, but in each case, the apparent ages in the high-temperature extractions (where the bulk of the cosmogenic Ar is released) are >1000 Ma, so it is possible that the cosmogenic Ar was not completely degassed in the events that partially reset the K–Ar system.

5. Discussion

The origin of the nonmare material in the Apollo 12 regolith is not known in detail. The site is nominally a mare site because mare volcanics cover nonmare material of the Fra Mauro or related Alpes Formations. The regolith, nevertheless, consists of about 43% nonmare material (<1-mm fines; Korotev et al., 2000). The composition of the nonmare component of the Apollo 12 regolith is similar to that of the Apollo 14 regolith. This similarity is not surprising because the Apollo 14 site is only 180 km to the east on the Fra Mauro Formation. It is reasonable to expect that some of the nonmare component of the Apollo 12 regolith derives from impacts that penetrate the basalts and exhume underlying and perhaps interlayered nonmare material (i.e. "vertical mixing") (Rhodes, 1976). The basalts at the site are some 300 m thick (DeHon, 1979), so vertical mixing may have proceeded in part by impacts that occurred during the intervals of basaltic volcanism in the region (Jolliff et al., 2000). Exposures of Alpes Formation (nonmare) occur within 50 m of the landing site, so it is also reasonable to expect that "lateral mixing" by many impacts into adjacent nonmare areas has also delivered nonmare material to the site over this distance. However, Clementine data suggest that such mixing is efficient only within 10–20 km of the contact (Jolliff et al., 2000; Li and Mustard, 2000, 2003). Finally, ejecta from the large craters Copernicus and probably Reinhold (Fig. 1A) occur at the site. Ejecta from the Upper Imbrian crater Lansberg are buried by the youngest basalts at the Apollo 12 site, but perhaps they occur in a paleoregolith at some depth less than the full 300 m thickness of basalts at the site. However, crater-ejecta models do not account for addition of as much as 43% material at the Apollo 12 site solely as ejecta from these three craters (Jolliff et al., 2000).

Regardless, the Apollo 12 regolith contains a large fraction of nonmare materials. A goal of this study is to provide some insights on the source of these nonmare materials. Following is a discussion of the Ar–Ar geochronology results of samples used in this study.

5.1. Plateau ages

Plateau ages are considered here as three or more consecutive steps that release 60% or more of the ^{39}Ar with apparent ages overlapping within their 1-σ error. Only a few samples dated by Ar–Ar geochronology in this work yielded plateau ages. Sample 12037,225-03 is a KREEP impact-melt breccia, and a split of this sample yielded a plateau age of 3991 ± 25 Ma (Fig. 4-13). This is the only impact-melt breccia of the set of samples that gave a plateau age. Although this age (pre-Imbrium) is older than other impact-melt breccia fragments (e.g., samples 12033,634-18 and 12033,634-24) we cannot assign any major significance to this result because we could not reproduce this age in the other split (Fig. 4-14) and in the other impact-melt breccias. Further work is needed in order to properly evaluate if some other impact-melt breccias from the Apollo 12 landing site are actually pre-Imbrium in age.

Samples 12001,911-01, 12023,146-02, 12024,074-04, and 12070,882-02 are all impact-melt breccias with compositions consistent with 2-to-1 mixtures of KREEP or KREEP-rich regolith and mare basalt. Plateau ages were obtained for samples 12023,146-02 (Fig. 4-18) and a split of sample 12024,074-04 (Fig. 4-19), which are ~1059 and 1054 Ma, respectively (Table 2). Sample 12001,911-01 did not yield a plateau sensu stricto, but 65% of ^{39}Ar was released in a single step with an associated age of 1575 Ma. These samples likely formed locally in impacts large enough that the melt volume was mainly below the veneer of mare basalt. The mare component may be largely clastic. Although these three samples have very similar compositions (Table 1), they come from three different sample locations (Fig. 1 and Table 1), which could explain the different ages. Another possible explanation is that these plateau ages actually represent partial degassing ages and the actual formation age is much older.

Regarding the alkali anorthosite sample 12033,634-06, the ^{40}Ar/^{39}Ar analyses yielded a plateau age of 3256 ± 22 Ma. This age is the youngest so far determined for a lunar anorthosite. Analysis of another alkali anorthosite (sample 12001,907-05) did not yield a plateau age, but 11 consecutive steps with approximately 68% of the ^{39}Ar yielded a weighted average of 3105 ± 58 Ma. Previous geochronology on lunar alkali anorthosites have yielded ages between 4.34 and 4.02 Ga (e.g., Lunatic Asylum, 1970; Turner, 1971; Shih et al., 1993; Meyer et al., 1996). Meyer et al. (1989) provided U–Pb zircon ages for two alkalic Apollo 14 rocks. Sample 14321,16 (alkali anorthosite) yielded an age of 4028 ± 6 Ma and sample 14066,47 (alkali gabbronorite) gave an age of 4141 ± 5 Ma. These authors also analyzed a zircon from an Apollo 16 alkali gabbronorite, obtaining an age of 4339 ± 5 Ma. Snyder et al. (1995) analyzed two fragments of alkali affinity from the Apollo 14 collection using Sm–Nd and Rb–Sr systematics, and obtained a four point Sm–Nd isochron of 4108 ± 53 Ma on an alkali anorthosite (sample 14304,267). Rb–Sr determination on the same sample yielded an errorchron (MSWD > 4) with an age of 4336 ± 81 Ma. On the basis of these results, Snyder et al. (1995) concluded that alkalic magmatism occurred over an extended period of time (~300 Myr) from 4.34 to 4.02 Ga and suggested an origin of the alkali suite as cumulates from KREEP-basalt melts.

If the ^{40}Ar/^{39}Ar ages obtained here for the Apollo 12 alkali anorthosites represent the crystallization ages, then an origin of these alkali anorthosites as magmatic differentiates of KREEP basalt parent magmas is unlikely on the basis of published KREEP basalt ages. On the other hand, Hawke et al. (2003) identified anorthosites within the Procellarum region using telescopic near-infrared spectra and multispectral images from the Galileo and Clementine missions. Hawke et al. (2003) proposed that these anorthosites could result from extended differentiation of Mg-suite plutons. The products of this magmatism (i.e., granites, quartz monzodiorites, alkali anorthosites, and alkali norites and gabbros) could have reached the Apollo 12 landing site by lateral and/or vertical mixing following impacts into the source rocks. Such rocks do occur at the Apollo 12 landing site as well as at the Apollo 14 landing site, even if only as small rock fragments (Jolliff et al., 1991). A second possibility is that these ages represent complete resetting of the argon systematics in a ~3.2 Ga impact event.

5.2. Degassing/resetting ages

Most of the samples analyzed here show some degree of degassing at around 700–800 Ma (Fig. 5). This characteristic is particularly evident in samples 12023,145-03 (Fig. 4-4), 12032,366-13 (Fig. 4-5), -30 (Fig. 4-6 and -7), 12033,634-04 (Fig. 4-8), -07 (Fig. 4-9), -15 (Fig. 4-10), -24 (Fig. 4-11), -26 (Fig. 4-12), -18 (Fig. 4-16) and 12070,882-02 (Fig. 4-21), which are all KREEP-bearing lithologies. Degassing at 700–800 Ma is also observed in the two felsite samples: sample 12032,366-07 (Fig. 4-3), and in both splits of sample 12001,912-02 (Fig. 4-1 and -2). Minimum formation ages for the samples that show partial degassing at 700–800 Ma range from ~1.0 Ga (sample 12032,366-07) to ~3.1 Ga (sample 12032,366-41A), with most concentrated in the 2.0–2.3 Ga range. Looking at the data in more detail, we find nine of the 27 samples or splits have plateaus (or at least weighted averages of similar points) between 663 and 822 Ma, with another at 860 Ma. Four ages range between 769 and 792 and overlap within errors. These samples yielded a weighted average of 789 ± 13 Ma, which overlaps with the 800 ± 15 Myr age given by Bogard et al. (1994) for Copernicus crater. Four samples give younger ages of 663 ± 17, 685 ± 8, 688 ± 10, and 706 ± 6 Ma, which may reflect a younger degassing event. Two other samples have older ages of 822 ± 60 and 862 ± 38 Ma, which overlap within errors and which may reflect an older degassing event (Fig. 5). An analyses of the lower-limit age of all samples show that 11 samples have minimum ages between 700 and 805 Ma, and yields a weighted average of 782 ± 21 (1-σ), which we adopt as our best estimate of the time of some important event at the Apollo 12 site (Table 2).

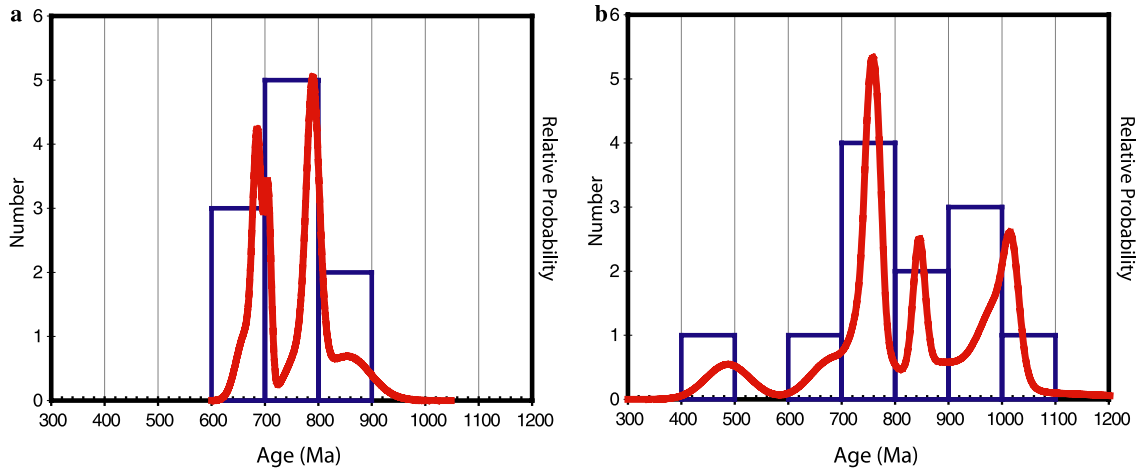

Fig. 5. Probability density plots for degassing/resetting ages. (a) Plot for samples that yielded a plateau age or weighted averages of similar points, main peaks at 790 and 686 Ma; (b) plot for samples with minimum ages less 1.1 Ga and that did not yield young age plateaus or weighted averages.

The consistent degassing age of 700–800 Ma observed in most of the samples is concordant with previous geochronological studies on Apollo 12 KREEP-rich soils. Eberhardt et al. (1973) inferred an age of 800 ± 40 Ma for Copernicus based on Ar–Ar analyses of two separates from sample 12033. Similarly, Alexander et al. (1976) suggested an age for Copernicus of $800 + 400, -50$ Ma. Meyer et al. (1996), using U-Pb systematics on four zircons from a granite fragment from sample 12033,507, obtained crystallization ages of ~3.9 Ga, with two analyses showing disturbance at $\sim 760 \pm 200$ Ma. Later, Bogard et al. (1994) obtained an age of 800 ± 15 Ma for a granite fragment from sample 12033,507. This degassing age has been interpreted as the most precise age determination for the Copernicus impact event (Bogard et al., 1994). On the other hand, a recent study of Apollo 12 glass spherules by Levine et al. (2005) shows that most have ages less than 500 Ma. In another study on impact-melt glasses from the Apollo 14 and 17 landing sites, Zellner et al. (2006) concluded that a transient increase in the impact flux occurred at ~800 Ma.

The results presented here suggest that many samples at the Apollo 12 site carry the same age signature. This signature could have been embedded on the landing site from the hot ejecta associated with the Copernicus impact event that caused the thermal resetting of the Ar systematics. Estimates of the ejecta deposit formed by the Copernicus event at the Apollo 12 landing site suggest addition of around 0.45 m equivalent thickness of material, calculated using the mathematical expression in Melosh (1989). The resetting at the Apollo 12 site appears to have been more widespread than might have been expected.

To reset the K–Ar system, the temperature of a rock has to be elevated over its closing temperature for a sufficient period. In most impacts, far more material is transported or disturbed than is heated sufficiently to have its K–Ar system reset. Hence, if the material at the Apollo 12 landing site is in part Copernicus ejecta, we would not necessarily expect it to have reset ages. Alternatively, an impact can cause age resetting by emplacing ejecta that is hot enough (or deposits enough energy) to heat the regolith underneath it. But at this distance from Copernicus, we would expect ejecta deposition to be ballistic, and to result in more churning and mixing than heating. One possibility is that because the Apollo 12 site is within a ray of Copernicus, this led to more substantial heating effects than would otherwise occur. Another possibility is that these resetting ages do not all reflect the influence of Copernicus. Concentrations of apparent impact resetting ages of 700–800 Ma have also been seen in some Apollo 14, 16, and 17 glass spherules (Zellner et al., 2005, 2006), other lunar samples (Delano, personal communication), and some L chondrite meteorites (Kring et al., 1996), so these ages may reflect or have been a part of some larger series of impact events clustered in this time interval.

If we apply the same equation for determining the ejecta deposit contribution (Melosh, 1989) of Lansberg and Reinhold at the Apollo 12 site, we find that about 0.91 and 0.30 m equivalent thickness of material on average, would have been added from these two craters, respectively. Although those materials were buried by the youngest basalt flows at the Apollo 12 site, they may be present in the surface regolith as a result of impact gardening over the past 3 Ga. It is thus possible that the nonmare material found in the Apollo 12 regolith is a mixture from these three different craters, namely Copernicus, Reinhold, and Lansberg; however, we do not see in the age data any indication of clustering of older resetting ages that might correspond to the older craters. Instead, it appears that the 700–800 Ma age signature imparted by the Copernicus ejecta and/or other Copernican impact event(s) dominates the $^{40}Ar/^{39}Ar$ geochronological data.

6. Conclusions

The most notable conclusion of this work is that most samples analyzed here show some degree of degassing during the interval 700–800 Ma, with a best estimate of

782 ± 21 Ma (1-σ). This age overlaps, within error, the degassing age of ~800 Ma reported for a lunar granite fragment of sample 12033,507 that has been interpreted as the age of Copernicus (Bogard et al., 1994). The data reported here suggest that most of the nonmare materials are affected by a ~700–800 Ma event, presumably the Copernicus impact and ejecta, but possibly as part of some other impact event or series of events associated with an increase in the impact flux at ~800 Ma as visualized by Zellner et al. (2006).

Two alkali anorthosite samples yielded ages of 3256 ± 22 Ma (plateau age) and 3105 ± 58 Ma (weighted average age). We interpret this age as the crystallization age of the fragments. These are coincidentally similar to crystallization ages for basalts from the Apollo 12 site (Stöffler and Ryder, 2001 and references therein). These crystallization ages are the youngest age so far determined for lunar anorthosites, so we suspect they may be related to late differentiation processes associated with relatively young magmatic activity. A pre-Imbrium age (~3.99 Ga) was determined for an impact-melt breccia, but it is not clear if this age has any real implications or if it represents an outlier (for example, as a result of an undegassed clast). Further work is necessary to properly evaluate the presence of pre-Imbrium nonmare material at this site and its implications.

Acknowledgments

This contribution is dedicated to the memory of Larry Haskin Support for this research comes from NASA Cosmochemistry Grants NAG5-12059 (T.S) and NNG04GG10G (R.K), and Planetary Geology and Geophysics Grant NNG05GI38G (B.J). This manuscript has benefited from constructive reviews by Vera Fernandes, Ray Burgess, and an anonymous reviewer. Editorial comments and suggestions by Rainer Wieler are appreciated.

Associate editor: Rainer Wieler

Supplementary data

Supplementary data associated with this article can be found, in the online version, at doi:10.1016/j.gca.2006.09.013.

References

Alexander Jr., E.C., Bates, A., Coscio Jr., M.R., Dragon, J.C., Murthy, V.R., Pepin, R.O., Venkatesan, T.R., 1976. K/Ar dating of lunar soils II. *Proc. Lunar Sci. Conf.* **7**, 625–648.

Alexander Jr., E.C., Davis, P.K., 1974. ^{40}Ar–^{39}Ar ages and trace element contents on Apollo 14 breccias: an interlaboratory cross-calibration of ^{40}Ar–^{39}Ar standards. *Geochim. Cosmochim. Acta* **38**, 911–928.

Barra, F., Swindle, T.D., Korotev, R.L., Jolliff, B.L., Zeigler, R.A., Olson, E.K., 2004. ^{40}Ar–^{39}Ar geochronology of Apollo 12 regolith. *Lunar Planet. Sci.* XXXV. Lunar Planet. Inst., Houston. #1365 (abstr.).

Bogard, D.D., Garrison, D.H., McKay, D.S., Wentworth, S.J., 1992. The age of Copernicus: new evidence for 800 ± 15 million years. *Lunar Planet. Sci.* **23**, 133–134.

Bogard, D.D., Garrison, D.H., Shin, C.-Y., Nyquist, L.E., 1994. ^{39}Ar–^{40}Ar dating of two lunar granites: the age of Copernicus. *Geochim. Cosmochim. Acta* **58**, 3093–3100.

Cohen, B.A., 2000. Geochemistry and Argon 40–Argon 39 Geochronology of Lunar Meteorite Impact Melt Clasts. Ph. D. thesis, University of Arizona.

Compston, W., Berry, H., Vernon, M.J., Chappell, B.W., Kaye, M.J., 1971. Rubidium–strontium chronology and chemistry of lunar material from the Oceans of Storms. *Proc. Lunar Sci. Conf.* **2**, 1471–1485.

DeHon, R.A., 1979. Thickness of the western mare basalts. *Lunar Planet. Sci.* **10**, 2935–2955.

Eberhardt, P., Geiss, J., Graf, H., Grögler, N., Mendia, M.D., Mörgeli, M., Stettler, A., Krähenbühl, U., von Gunten, H.R., 1972. Trapped solar wind noble gases in Apollo 12 lunar fines 12001 and Apollo 11 breccia 10046. *Proc. Lunar Sci. Conf.* **3**, 1821–1856.

Eberhardt, P., Geiss, J., Grögler, N., Stettler, A., 1973. How old is the crater Copernicus? *The Moon* **8**, 104–114.

Eugster, O., Terribilini, D., Polnau, E., Kramers, J., 2001. The antiquity indicator argon-40/argon-36 for lunar surface samples calibrated by uranium-235–xenon-136 dating. *Meteorit. Planet. Sci.* **36**, 1097–1115.

Gnos, E., Hofmann, B.A., Al-Kathiri, A., Lorenzetti, S., Villa, I., Eugster, O., Jull, A.J.T., Eikenberg, J., Spettel, B., Krähenbühl, U., Franchi, I.A., Greenwood, G.C., 2003. Lunar meteorite SaU 169: An extremely KREEP-rich rock. *Meteorit. Planet. Sci.* **38**, A40.

Hawke, B.R., Peterson, C.A., Blewett, D.T., Bussey, D.B.J., Lucey, P.G., Taylor, G.J., Spudis, P.D., 2003. Distribution and modes of occurrence of lunar anorthosite. *J. Geophys. Res.* **108** (E6), 5050.

Hohenberg, C.M., Marti, K., Podosek, F.A., Reedy, R.C., Shirck, J.R., 1978. Comparisons between observed and predicted cosmogenic noble gases in lunar samples. *Lunar Planet. Sci.* **9**, 2311–2344.

Horn, P., Jessberger, E.K., Kirsten, T., Richter, H., 1975. ^{39}Ar–^{40}Ar dating of lunar rocks: effects of grain size and neutron irradiation. *Proc. Lunar Sci. Conf.* **6**, 1563–1591.

Hubbard, N.J., Meyer Jr., C., Gast, P.W., Wiesmann, H., 1971. The composition and derivation of Apollo 12 soils. *Earth Planet. Sci. Lett.* **10**, 341–350.

Jolliff, B.L., 1991. Fragments of quartz monzodiorite and felsite in Apollo 14 soil particles. *Lunar Planet. Sci.* **21**, 101–118.

Jolliff, B.L., Gillis, J.L., Korotev, R.L., Haskin, L.A., 2000. On the origin of nonmare materials at the Apollo 12 landing site. *Lunar Planet. Sci.* XXXI. Lunar Planet. Inst., Houston. #1671 (abstr.).

Jolliff, B.L., Korotev, R.L., Haskin, L.A., 1991. Geochemistry of 2–4 mm particles from Apollo 14 soil (14161) and implications regarding igneous components and soil-forming processes. *Lunar Planet. Sci.* **21**, 193–219.

Jolliff, B.L., Rockow, K.M., Korotev, R.L., Haskin, L.A., 1996. Lithologic distribution and geologic history of the Apollo 17 site: the record in soils and small rock particles from the highland massifs. *Meteorit. Planet. Sci.* **31**, 116–145.

Jolliff, B.L., Zeigler, R.A., Korotev, R.L., Barra, F., Swindle, T.D., 2005. A thorium-rich mare basalt rock fragment from the Apollo 12 regolith: A sample from a young Procellarum flow? *Lunar Planet. Sci.* XXXVI. Lunar Planet. Inst., Houston. #2357 (abstr.).

Korotev, R.L., 1997. Some things we can infer about the Moon from the composition of the Apollo 16 regolith. *Meteorit. Planet. Sci.* **32**, 447–478.

Korotev, R.L., Jolliff, B.L., Zeigler, R.A., 2000. The KREEP components of the Apollo 12 regolith. *Lunar Planet. Sci.* XXXI. Lunar Planet. Inst., Houston. #1363 (abstr.).

Korotev, R.L., Rockow, K.M., 1995. Compositional trends in Apollo 12 soils. *Lunar Planet. Sci.* **26**, 787–788.

Korotev, R.L., Zeigler, R.A., Jolliff, B.L., Haskin, L.A., 2002. Lithologies of the Apollo 12 regolith. *Lunar Planet. Sci.* XXXIII. Lunar Planet. Inst., Houston. #1395 (abstr.).

Kring, D.A., Swindle, T.D., Britt, D.T., Grier, J.A., 1996. Cat Mountain: a meteoritic sample of an impact-melted asteroid regolith. *J. Geophys. Res.* **101** (E12), 29353–29372.

Levine, J., Becker, T.A., Muller, R.A., Renne, P.R., 2005. ^{40}Ar/^{39}Ar dating of Apollo 12 glass spherules. Geophys. Res. Lett. **32**, doi:10.1029/2005GL022874.

Li, L., Mustard J.F., 2000. Compositional gradients across mare-highland contacts: importance and geological implication of lateral transport. *J. Geophys. Res.* **105** (20), 431–20,450.

Li, L., Mustard, J.F., 2003. Highland contamination in lunar mare soils: improved mapping with multiple end-member spectral mixture analysis (MESMA). *J. Geophys. Res.* **108**(E6) doi:10.1029/2002JE001917.

Ludwig, K., 2001. Users manual for Isoplot/Excel version 2.49. *A geochronological toolkit for Microsoft Excel*. Berkeley Geochronological Center Special Publication 1a.

Lunatic Asylum, 1970. Mineralogic and isotopic investigations on lunar rock 12013. *Earth Planet. Sci. Lett*. **9**, 137–163.

Melosh, H.J., 1989. *Impact Cratering: A Geological Process*. Oxford University Press, Oxford.

Meyer, C., Williams, I.S., Compston, W., 1989. $^{207}Pb/^{206}Pb$ ages of zircon-containing rock fragments indicate continuous magmatism in the lunar crust from 4350 to 3900 million years. *Lunar Planet. Sci.* **20**, 691–692.

Meyer, C., Williams, I.S., Compston, W., 1996. Uranium-lead ages for lunar zircons: evidence for a prolonged period of granophyre formation from 4.32 to 3.88 Ga. *Meteorit. Planet. Sci.* **31**, 370–387.

Neal, C.R., Hackker, M.D., Snyder, G.A., Taylor, L.A., Liu, Y.-G., Schmitt, R.A., 1994. Basalt generation at the Apollo 12 site, Part 2: source heterogeneity, multiple melts, and crustal contamination. *Meteoritics* **29**, 349–361.

Nyquist, L.E., Bansal, B.M., Wooden, J.L., Wiesmann, H., 1977. Sr-isotopic constraints on the petrogenesis of Apollo 12 mare basalts. *Lunar Planet. Sci.* **8**, 1383–1415.

Nyquist, L.E., Shih, C.-Y., Wooden, J.L., Bansal, B.M., Wiesmann, H., 1979. The Sr and Nd isotopic record of Apollo 12 basalts: implications for lunar geochemical evolution. *Lunar Planet. Sci.* **10**, 77–114.

Nyquist, L.E., Wooden, J.L., Shih, C.-Y., Wiesmann, H., Bansal, B.M., 1981. Isotopic and REE studies of lunar basalt 12038: implications for petrogenesis of aluminous mare basalts. *Earth Planet. Sci. Lett.* **55**, 335–355.

Papanastassiou, D.A., Wasserburg, G.J., 1971. Lunar chronology and evolution from Rb–Sr studies of Apollo 11 and Apollo 12 samples. *Earth Planet. Sci. Lett.* **11**, 37–62.

Rhodes, J.M., 1976. Some compositional aspects of lunar regolith evolution. *Philos. Trans. R. Soc. Lond.* **A285**, 293–301.

Shih, C.-Y., Nyquist, L.E., Wiesmann, H., 1993. K–Ca chronology of lunar granites. *Geochim. Cosmochim. Acta* **57**, 4827–4841.

Shoemaker, E.M., Batson, R.M., Bean, A.L., Conrad, Jr. C., Dahlem, D.H., Goddard, E.N., Hait, M.H., Larson, K.B., Schaber, G.G., Schleicher, D.L., Sutton, R.L., Swann, G.A., Waters, A.C., 1970). Preliminary geologic investigations of the Apollo 12 landing site. In: *Apollo 12 Preliminary Science Report*, NASA Spec. Publ. SP-235, Manned Spacecraft Center, Houston, Texas. pp. 113–182.

Snyder, G.A., Taylor, L.A., Halliday, A.N., 1995. Chronology and petrogenesis of lunar highlands alkali suite: cumulates from KREEP basalt crystallization. *Geochim. Cosmochim. Acta* **59**, 1185–1203.

Stettler, A., Eberhardt, P., Geiss, J., Grögler, N., Maurer, P., 1973. ^{39}Ar–^{40}Ar ages and ^{37}Ar–^{38}Ar exposure ages of lunar rocks. *Proc. Lunar Sci. Conf.* **4**, 1865–1888.

Stöffler, D., Ryder, G., 2001. Stratigraphy and isotope ages of lunar geologic units: chronological standard for the inner Solar System. *Space Sci. Rev.* **96**, 9–54.

Swindle, T.D., Olson, E.K., 2004. ^{40}Ar–^{39}Ar studies of whole rock nakhlites: evidence for the timing of formation and aqueous alteration on Mars. *Meteorit. Planet. Sci.* **39**, 755–766.

Turner, G., 1971. ^{40}Ar–^{39}Ar ages from the lunar maria. *Earth Planet. Sci. Lett.* **11**, 169–191.

Warner, J., 1970. Apollo 12 lunar-sample information. NASA Technical Report R-353, Manned Spacecraft Center, Houston, Texas. p. 386.

Warren, P.H., 1989. KREEP: Major-element diversity, trace-element uniformity (almost). In: Taylor G.J., P.H. Warren (Eds.), *Workshop on Moon in Transition: Apollo 14, KREEP, and Evolved Lunar Rocks*. LPI Tech. Report 89-03, pp. 149–153. Lunar and Planetary Institute, Houston.

Wilhelms, D.E., 1987. The *Geologic History of the Moon*. U.S. Geol. Surv. Prof. Paper 1348.

Zeigler, R.A., Korotev, R.L., Haskin, L.A., Jolliff, B.L., Gillis, J.J., 2006. Petrology and geochemistry of five new Apollo 16 mare basalts and evidence for post-basin deposition of basaltic material at the site. *Meteorit. Planet. Sci.* **41**, 263–284.

Zellner, N.E.B., Delano, J.W., Swindle, T.D., Barra, F., Olson, E.K., Whittet, D.C.B., Spudis, P.D., 2005. Earth–Moon impacts at ~300 Ma and ~500 Ma ago. *Lunar Planet. Sci.* XXXVI. Lunar Planet. Inst., Houston. #1204 (abstr.).

Zellner, N.E.B., Delano, J.W., Swindle, T.D., Barra, F., Olson, E.K., Whittet, D.C.B., 2006. Did a transient increase in the impact flux occur 800 Ma ago? *Lunar Planet. Sci.* XXXVII. Lunar Planet. Inst., Houston. #1745 (abstr.).